# Response to Referee #1

We sincerely thank the editor and all reviewers for your time and the constructive comments on our manuscript. We have carefully considered all the comments and suggestions. Below are our point-by-point detailing how we have addressed each issue in the revised manuscript. In the following, paragraphs in **black** are reviewers' comments; paragraphs in **blue** are point-to-point responses; paragraphs in **red** are revisions in the manuscript.

# General Comments:

The paper addresses a relevant question: Can a large-aperture scintillometer be used for accurate measurements of aerosol mass fluxes over open water? The experimental set-up of using EC and dry deposition filters seems appropriate to answer this question. However, in the way the method is executed and the data is analyzed, quite some issues come forward that must be addressed.

Before responding point by point, we wish to explain a fundamental restructuring of the manuscript prompted by Reviewer 2's concern about the PWD50. Although the PWD50 output was logged at 1 Hz, the standard instrument has an independent measurement interval of 15 s; therefore, the 1 s records cannot be treated as independent fast-response extinction observations. Our reanalysis of the four campaigns, including vertical-wind–extinction co-spectra and cumulative ogives, did not show a stable and reproducible turbulent covariance that could support a conventional aerosol eddy-covariance flux. We consequently removed the entire LAS–EC comparison and the associated argument that agreement with EC demonstrated the feasibility of LAS. The PWD50 is now used only as a low-time-resolution visibility/extinction reference for the hourly $R_{MN}$ calibration and for reproducible fog screening. The revised manuscript instead extends the LAS framework from terrestrial to open-water-dominated environments from the theoretical and measurement perspectives: it evaluates the separation of the real and imaginary refractive-index contributions in the LAS spectrum, introduces campaign-specific continuous $R_{MN}$ (RH) relationships, and retrieves aerosol mass-flux magnitudes. Accordingly, the revised claims are restricted to path-integrated aerosol mass-exchange magnitudes and their temporal variability under the stated operating conditions; independent EC validation is no longer claimed.

## Specific Comments:

**Major Comment 1:** The dry deposition filters for measuring the aerosol mass, used for determining the aerosol fluxes, are handled in ways that do not seem to comply with European or American standards. See https://www.nature.com/articles/s41598-026-42411-4 for a paper that explicitly mentions these standards. The authors should indicate what kind of standard they follow with their method and how this method or standard relates to the European or American standards for measuring particulate matter. Of particular concern is the condensation of gaseous organic carbons, see https://acp.copernicus.org/articles/9/7243/2009/.

**Response:** We thank the reviewer for pointing out this critical detail and for providing the highly relevant references. To clarify, the parameter of "45 ± 1 ℃ for 3 hours" mentioned in the original manuscript was not the final equilibration condition. Rather, it was a pre-conditioning step designed to establish a stable dry baseline for open-water samples. Following the pre-conditioning step, the actual equilibration and weighing process followed the Chinese National Standard (HJ 618-2011). The filters were equilibrated in a climate-controlled chamber set to and relative humidity (RH) for at least 24 hours prior to weighing. We have revised the manuscript to clearly distinguish this standard equilibration step from the pre-drying step. Samples collected over open water experience generally high humidity conditions, especially over the sea surface. The 45 ℃ step ensures that all samples are reset to a uniform, consistent dry baseline before entering the 20 ℃/50% RH standard environment. The same conditioning, blank correction, repeated weighing, and concentration-calculation procedures were applied to the $PM_{2.5}$ and $PM_{10}$ filters collected with the corresponding size-selective impactors.

Furthermore, we appreciate the reviewer raising the specific concern regarding the condensation of gaseous organic carbons. It is well-documented in the literature that the adsorption or condensation of ambient gaseous organics onto the filter matrix introduces a positive artifact (Kirchstetter et al., 2001; Cheng et al., 2009). For instance, Cheng et al. reported that this artifact can lead to an artificial overestimation of the particulate organic carbon (OC) mass by 8% to 66%. We acknowledge that since our setup employed single bare filters without an organic denuder, this positive artifact cannot be excluded. However, in open-water especially marine environments, the total aerosol mass is overwhelmingly dominated by inorganic components. Taking sea spray aerosols with dry diameters greater than 1 μm as an example, inorganic sea salts account for 99% of the mass (Quinn et al., 2015). Consequently, even if the minor OC fraction experienced the maximum 66% overestimation reported by Cheng et al., its contribution to the absolute measurement error of the total aerosol mass would remain limited relative to the total aerosol mass. We now acknowledge the potential influence of gaseous organic compound adsorption onto the bare glass-fiber filters.

**The Sect. 2.1, Pages 4-5, lines 108-124:**

"Filter-based aerosol sampling was also conducted during the four field campaigns…Potential biases from semi-volatile particle loss during heating and adsorption of gas-phase organic compounds on the bare glass-fiber filters cannot be excluded."

**Major Comment 2:** The use of 30 min intervals, 2 hour intervals, (moving) averages, and outlier rejection greatly impacts the statistical analyses used by the authors. Stating that the correlation for a 30 min interval is low and that the deviation between 2hr averages is also low, seems more like an application of the Central Limit Theorem than an actual physical result. This also impacts the ensemble averages, but there the averages become more problematic due to the large spread (2 orders of magnitude) of the aerosol fluxes. In those cases the average of the logarithmic values (the geometric mean) or the use of the median would be more appropriate. Since the authors already calculate and display the median, they would do well to redo their analysis and conclusions based on the median values for the ensemble. Regarding the selection bias, the authors clearly show that removing data due to fog and rain impacts the comparison. Instead of seeing this as a reason to do follow-up analysis where the exact same selection was applied to the measurements, they weaken their conclusions and caution the reader for doing this. The authors should apply identical selections to the measurements in order to attain results from which stronger conclusions can be attained.

**Response:** We thank the reviewer for this comment. The statistical comparison discussed in the original manuscript has been removed. Specifically, all 30 min LAS–EC correlations, 2 h block averages, NRMSE values, pooled comparisons, and ensemble-mean EC/LAS cycles have been deleted because the PWD50 cannot provide independent fast-response extinction measurements. Consequently, improved agreement after temporal smoothing is no longer used as physical evidence.

We agree with the reviewer that the median is more appropriate for characterizing the central tendency of the broadly distributed flux magnitudes because it is less sensitive than the arithmetic mean to large values. The revised analysis uses the 30 min interval as the LAS retrieval window. Campaign distributions are summarized by medians and interquartile ranges, and daytime/nighttime contrasts are based on medians.

To make the revised outcome self-contained, the campaign medians and spreads are stated here. At Siyuan Lake, the median flux magnitudes were 0.091 and 0.123 μg $m^{-2}$ $s^{-1}$, with interquartile ranges of 0.058–0.150 and 0.075–0.231 μg $m^{-2}$ $s^{-1}$. At Sijiao Island, the corresponding medians were 0.399 and 0.114 μg $m^{-2}$ $s^{-1}$, with interquartile ranges of 0.174–0.936 and 0.073–0.161 μg $m^{-2}$ $s^{-1}$. These values use the accepted 30 min LAS retrievals; no smoothing-based agreement is used as evidence.

**The Sect. 2.7, Page 10, lines 241-244:**

"All measurements were processed at a common 30-min retrieval interval…data used to calibrate the aerosol mass-to-optical conversion."

**The Sect. 3.4, Page 22, lines 477-478:**

"At Siyuan Lake (Fig. 10), the campaign-median flux magnitudes were 0.091 and 0.123 μg $m^{-2}$ $s^{-1}$…0.075–0.231 μg $m^{-2}$ $s^{-1}$, respectively."

**The Sect. 3.4, Page 24, lines 509-510:**

"At Sijiao Island (Fig. 12), the campaign-median flux magnitudes were 0.399 and 0.114 μg $m^{-2}$ $s^{-1}$…0.073–0.161 μg $m^{-2}$ $s^{-1}$, respectively."

**Major Comment 3:** Lastly, the authors have done a comparison between LAS and EC before, but on land. The performance analysis of LAS versus EC at coastal environment should be compared with the same comparison for land environment. This is necessary to show the limitations of LAS, for which they now only give vague qualitative answers but no quantitative answers such as thresholds (for example the amount of attenuation by fog/particles where the LAS starts to give deviating answers, and thus data should be excluded) that allow reproduction by fellow scientists. Moreover, this manuscript contains the theory associated with land, while only fleetingly mentioning coastal influences.

**Response:** We agree with the reviewer's assessment. Because the EC route has been withdrawn, a numerical coastal-versus-terrestrial LAS–EC performance comparison is no longer an appropriate validation test. The terrestrial work is retained only as the methodological origin of the LAS retrieval framework. Building on the terrestrial LAS framework, we extended its theoretical treatment to open-water environments by explicitly accounting for the strong humidity dependence of the aerosol mass-to-optical conversion through campaign-specific continuous $R_{MN}$ (RH) relationships:

$$R_{MN} = R_{\mathrm{ref}}\left[\frac{1-RH/100}{1-RH_{\mathrm{ref}}/100}\right]^{\gamma}$$

where $R_{\mathrm{ref}}$ is the value of $R_{MN}$ at a reference humidity $RH_{\mathrm{ref}}$, and $\gamma$ characterizes the humidity dependence of the mass-to-optical relationship.

In the Siyuan Lake II 60–70 % RH example, 280 of 292 hourly pairs were retained, with $r = 0.87$ and $R_{MN} = 3835$ kg m$^{-3}$.

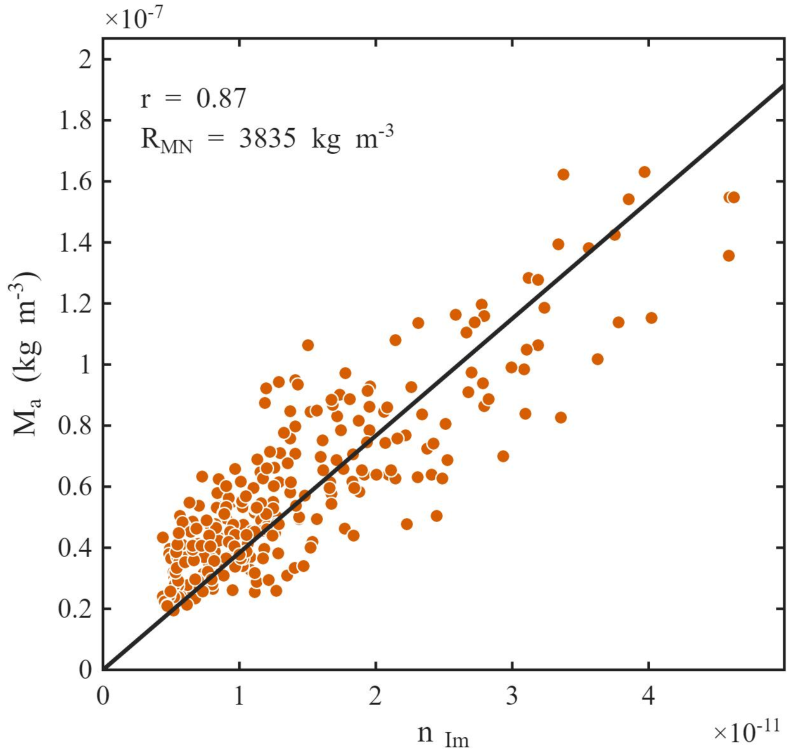


**Figure R1 (reproduced from the revised manuscript Fig. 5).** Example determination of $R_{MN}$ for the 60–70 % RH interval during Siyuan Lake II. Orange points denote the hourly aerosol mass concentration $M_a$ and the corresponding visibility-derived imaginary refractive index $n_{Im}$. The black line represents the linear regression of $M_a$ against $n_{Im}$.

Across the four campaigns, RH-bin regressions were retained only when the relationship between $PM_{10}$ and $n_{Im}$ was significant at $\alpha = 0.05$. The RH-bin estimates decreased with RH in every campaign, and the fitted $\gamma$ values were 0.750, 0.912, 1.518, and 0.838. Figure 7 is reproduced here because it shows the campaign-specific relationship that replaces the former constant conversion.

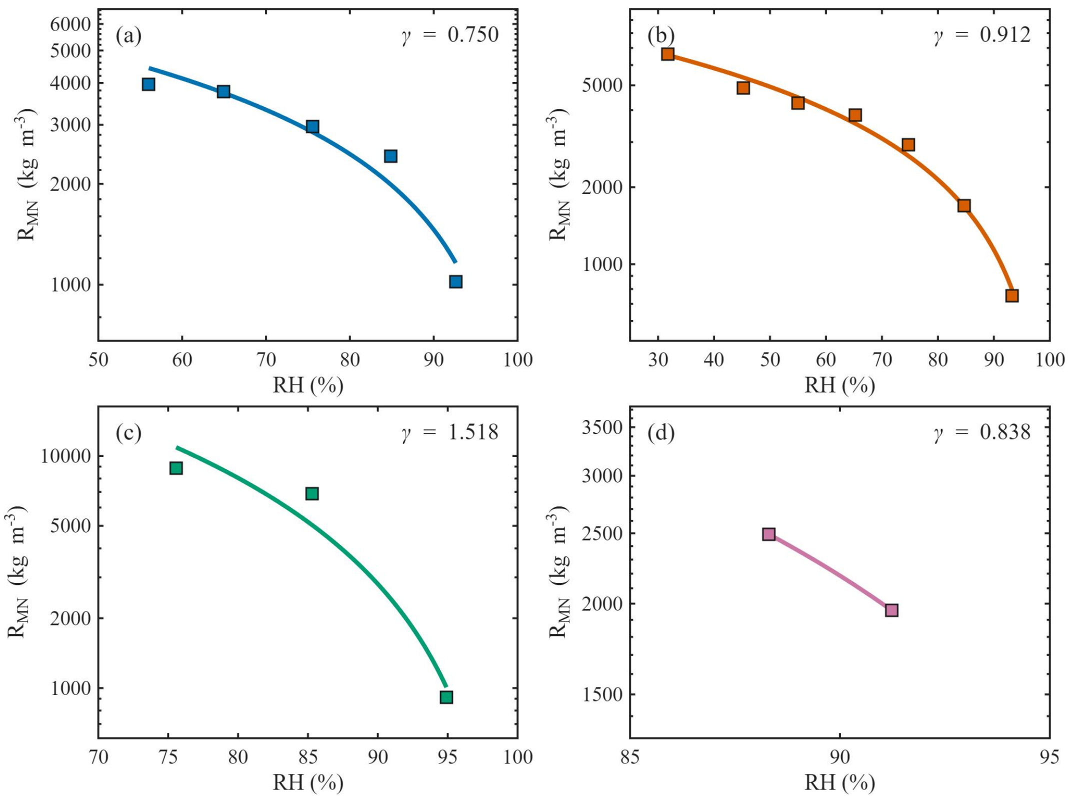


**Figure R2 (reproduced from the revised manuscript Fig. 6).** Variation of RH-bin $R_{MN}$ estimates during the four observational campaigns. Symbols denote the $R_{MN}$ estimates for individual RH intervals during Siyuan Lake I, Siyuan Lake II, Sijiao Island I, and Sijiao Island II, plotted at the nominal center of each RH bin; vertical bars show the corresponding 95 % confidence intervals.

We have replaced qualitative screening with reproducible thresholds. A 30 min LAS window requires at least 98 % raw coverage; it is rejected when the mean received voltage is below 0.005 V or below 2 % of the campaign-specific 90th-percentile reference, when rainfall exceeds 0.1 mm $h^{-1}$, when visibility is below 1 km, or when the spectral separation does not provide two resolved components and a crossover between 0.002 and 50 Hz. Table 3 reports the observed 5th–95th percentile operating ranges and the rejection outcomes for every campaign. Coastal influences are addressed explicitly through the continuous $R_{MN}$(RH) calibration, fog-related attenuation, and water-footprint fractions.

**Table R1 (reproduced from the revised manuscript Table 3).** Observed operating envelope, data availability, and rejection outcomes of the LAS aerosol-flux retrievals during the four campaigns.

| Metric | Siyuan Lake I | Siyuan Lake II | Sijiao Island I | Sijiao Island II |
|---|---|---|---|---|
| Mean wind speed ($m\ s^{-1}$) | 0.192–2.504 | 0.060–2.679 | 0.390–4.750 | 0.335–3.708 |
| Friction velocity ($m\ s^{-1}$) | 0.094–0.429 | 0.037–0.494 | 0.176–0.983 | 0.127–0.565 |
| Stability $\zeta$ | −0.704 to −0.007 | −1.516 to 0.509 | −0.612 to 0.072 | −0.720 to 0.123 |
| RH (%) | 59.11–89.98 | 28.59–87.02 | 71.62–97.16 | 85.87–92.52 |
| Extinction coefficient ($km^{-1}$) | 0.082–0.410 | 0.087–0.990 | 0.120–0.719 | 0.082–0.195 |
| Mean received-signal voltage (V) | 1.370–3.175 | 0.598–3.783 | 0.089–0.816 | 0.565–0.822 |
| Candidate intervals | 1,824 | 3,120 | 259 | 265 |
| Retained AERISP intervals, n (%) | 1,566 (85.9 %) | 2,612 (83.7 %) | 120 (46.3 %) | 261 (98.5 %) |
| Valid flux retrievals, n (%) | 1,531 (83.9 %) | 2,594 (83.1 %) | 119 (45.9 %) | 259 (97.7 %) |
| Precipitation rejection, n (%) | 234 (12.8 %) | 181 (5.8 %) | 0 | 0 |
| Fog rejection, n (%) | 0 | 43 (1.4 %) | 58 (22.4 %) | 0 |
| Received-signal rejection, n (%) | 3 (0.2 %) | 187 (6.0 %) | 32 (12.4 %) | 0 |
| Spectral/AERISP rejection, n (%) | 53 (2.9 %) | 113 (3.6 %) | 49 (18.9 %) | 4 (1.5 %) |
| Other QC rejection, n (%) | 3 (0.2 %) | 2 (0.1 %) | 1 (0.4 %) | 2 (0.8 %) |

*Note.* Environmental and signal ranges are the 5th–95th percentile ranges among final valid 30-min flux retrievals. Rejection categories are mutually exclusive and correspond to the first failed quality-control criterion.

**The Sect. 3.3, Pages 17-19, lines 379-429:**

"Conversion of $C_{n,\mathrm{Im}}^2$ to the aerosol mass-concentration structure parameter requires the mass-to-optical conversion…vertical bars show the corresponding 95 % confidence intervals."

**The Sect. 2.7, Page 10, lines 245-258:**

"For the LAS measurements, the original 500 Hz log-intensity signal was divided into consecutive 30-min windows…These criteria were applied consistently to all four campaigns."

**The Sect. 3.4, Pages 21-22, lines 458-469:**

"Final flux-retrieval availability was 83.9 %, 83.1 %, 45.9 %, and 97.7 %…rejection categories correspond to the first failed quality-control criterion."

**Minor Comment 1:** Figures 2 and 5 show transparent data points for the 30 min averages, while the 2 hr block values are shown non-transparent. The current transparency is so high that the 30 min average values are not seen as they are equally as bright as text on the other side of the paper seen through the paper. Suggestion: less transparent points or non-transparent points in other colors.

**Response:** We thank the reviewer for this comment. The figures referenced in this comment belonged to the former LAS–EC comparison and have been removed in full. The revised flux time-series figures display only the accepted 30 min LAS retrievals with opaque lines and explicit gaps at rejected intervals, so the transparency issue no longer arises. The two replacement time-series figures are reproduced below so that the reviewer can inspect the revised presentation within this response.

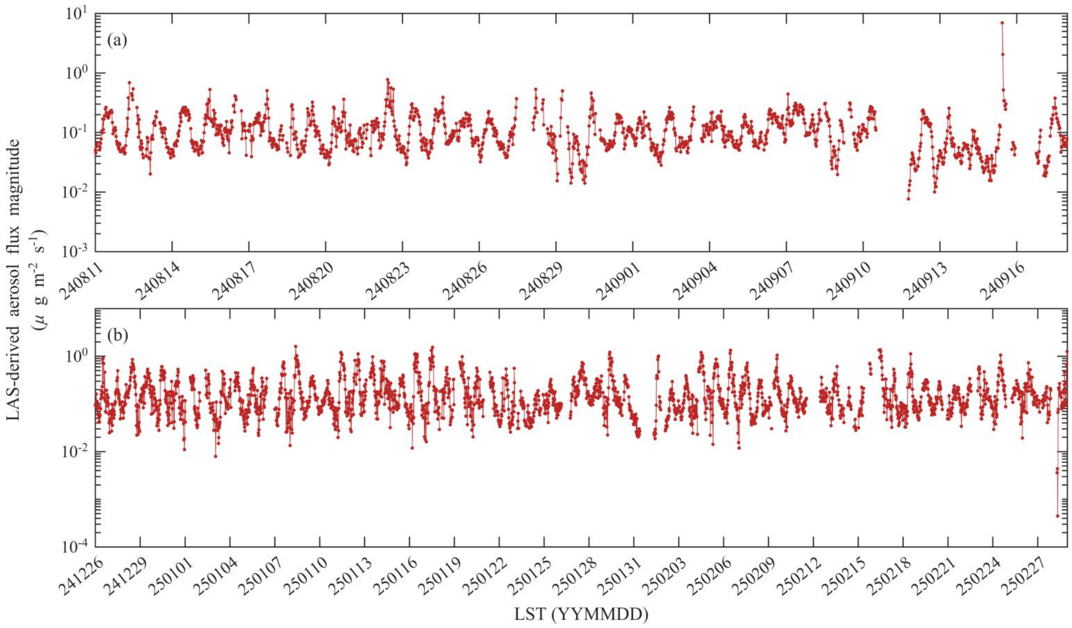


**Figure R3 (reproduced from the revised manuscript Fig. 10).** Temporal variations of the 30 min LAS-derived aerosol mass-flux magnitude during (a) Siyuan Lake I and (b) Siyuan Lake II. The vertical axis is logarithmic, and breaks denote intervals excluded by the quality-control criteria.

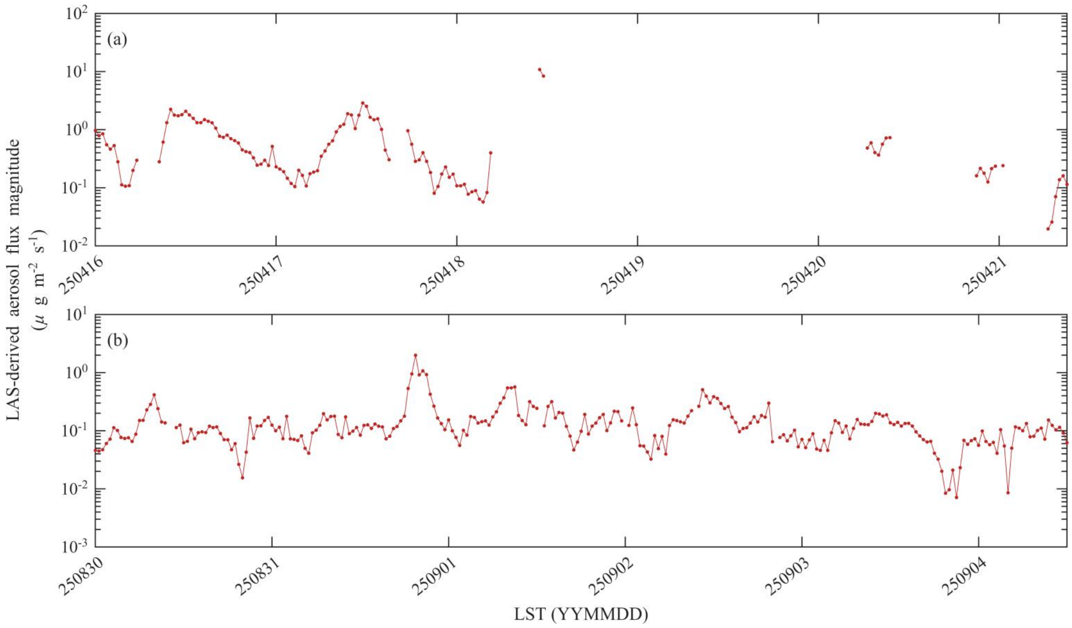


**Figure R4 (reproduced from the revised manuscript Fig. 12).** Temporal variations of the 30 min LAS-derived aerosol mass-flux magnitude during (a) Sijiao Island I and (b) Sijiao Island II. The vertical axis is logarithmic, and breaks denote intervals excluded by the quality-control criteria.

**The Sect. 3.4, Page 24, lines 499-501:**

"Figure 10. Temporal variations of the 30 min LAS-derived aerosol mass-flux magnitude…breaks denote intervals excluded by the quality-control criteria."

**The Sect. 3.4, Page 26, lines 535-537:**

"Figure 12. Temporal variations of the 30 min LAS-derived aerosol mass-flux magnitude…breaks denote intervals excluded by the quality-control criteria."

**Minor Comment 2:** Exclude the barbecue smoke data points.

**Response:** The barbecue-smoke event was localized near the point-based EC system and affected only the immediate vicinity of that instrument. It was therefore not considered to have materially influenced the LAS signal integrated over the entire optical path. Because the EC comparison has been removed, the affected EC points are no longer part of the revised analysis. Retention of each LAS interval is determined solely by the predefined optical, meteorological, spectral, and sonic-anemometer criteria in Sect. 2.7.

**Minor Comment 3:** Explain in the appendix better why the choice should be 30 min averages and not 1 hr averages, as the spectral behavior is minimal at 1 hr frequency.

**Response:** We thank the reviewer for this insightful comment. The original Appendix discussion concerned the averaging scale of the EC validation and has been removed together with that validation. In the revised method, 30 min is the retrieval interval used to estimate each LAS spectrum and its associated turbulence inputs. Given that both 30-min and 1-h periods are acceptable from a spectral perspective, we opted for the 30-min window primarily because it is the universally adopted standard in global flux networks (e.g., FLUXNET). Adhering to this convention helps our dataset to be directly comparable with mainstream micrometeorological studies. Additionally, utilizing a 30-min interval inherently provides a higher temporal resolution, yielding twice the amount of data points compared to a 1-h window.

**Minor Comment 4:** Explain why a gas analyzer was not associated with the EC system, and how its absence impacts the measurements.

**Response:** We thank the reviewer for this constructive suggestion, which has also provided useful guidance for upgrading our instrumentation in future campaigns. The revised manuscript contains no aerosol EC flux and therefore does not require a fast-response gas or particle analyzer for validation. The PWD50 is retained only for hourly visibility-derived extinction in the $R_{MN}$ calibration and for fog screening. The 20 Hz sonic anemometer is used independently to obtain friction velocity, Obukhov length, lateral-wind variability, and wind direction for the LAS flux and footprint calculations. In future deployments, we plan to complement the sonic anemometer with a fast-response gas analyzer and an independently characterized instrument capable of resolving high-frequency extinction or visibility fluctuations. Such a configuration would enable more complete EC measurements, determination of flux direction, and an independent evaluation of the LAS retrievals.

**Minor Comment 5:** Explain what kind of behaviors characteristic for coastal environments you expect to see with these measurements, and why these effects should be better or worse visible with an LAS system.

**Response:** We sincerely thank the reviewer for this insightful comment. Unlike inland water bodies, coastal aerosol fluxes may be influenced by dynamic mechanical forcings, such as wave breaking and bubble bursting, although the present study lacks the wave-state, aerosol-composition, and particle-size measurements needed to identify these mechanisms directly. Such surface processes can generate aerosol plumes that are episodic and spatially heterogeneous. While conventional single-point EC measurements are more susceptible to localized flux variability, the LAS integrates optical fluctuations along a long propagation path and therefore provides a spatially averaged measure of aerosol mass exchange. Although the EC-based calculation has been removed from the revised manuscript, this difference in spatial support remains relevant.

**Minor Comment 6:** Explain why the chosen set-up is chosen and not other set-ups like aerosol mass flux measurement instead of aerosol dry-deposition filtering method.

**Response:** We thank the reviewer for this methodological question. The broader objective of this series of LAS studies is to establish a quantitative link between an optical turbulence variable and an aerosol mass variable. In the present framework, the aerosol-related imaginary refractive-index fluctuations retrieved from the LAS log-intensity spectrum are converted, through $R_{MN}$, into aerosol mass-concentration fluctuations and ultimately into a path-averaged aerosol mass-flux magnitude. This optical-to-mass linkage is important because it expresses aerosol exchange in mass units relevant to atmospheric mass budgets and particulate-matter assessments, while retaining the spatial representativeness provided by the long LAS propagation path. It also avoids converting particle number to mass using additional assumptions concerning particle size, density, shape, and composition.

Common particle-counter-based eddy-covariance systems combine a fast-response condensation particle counter or optical particle counter with a three-dimensional sonic anemometer and primarily provide total or size-resolved particle-number fluxes. Because the LAS retrieval is expressed on a mass basis, the revised manuscript constructs a separate mass-based dry-deposition estimate from measured $PM_{2.5}$ and $PM_{10}$ concentrations and parameterized size-dependent deposition velocities over water. This calculation has the same flux units as the LAS result but represents a different physical process.

We agree that the dry-deposition calculation is not a direct flux measurement. It combines filter-derived aerosol concentrations with modeled deposition velocities and is used only as a process-based reference. The dry-deposition method is described in Sect. 2.6, the comparison is reported in Sect. 3.4, and the particle-size and density sensitivity is provided in Supplement Sect. S9, Tables S7a-S7b, and Fig. S11.

Future work could provide more direct and informative comparisons by deploying a fast-response CPC and/or a fast-response OPC/OPS together with a three-dimensional sonic anemometer to obtain particle-number and size-resolved EC fluxes. A fast-response aerosol extinction monitor, such as a cavity-attenuated phase-shift particle extinction monitor (CAPS $PM_{\mathrm{ex}}$), could additionally provide extinction fluctuations for an optical EC comparison. After applying the independently calibrated $R_{MN}$, both the extinction-based EC result and the LAS retrieval could be expressed on a mass basis, allowing their temporal response, flux direction, and point-versus-path spatial representativeness to be evaluated separately.

The revised comparison between LAS and dry-deposition calculation contains 41 filter samples matched to 154 valid 30 min LAS intervals. The Pearson correlation between the base-10 logarithms of the LAS and dry-deposition fluxes was 0.14 under the constant conversion and 0.53 under the RH-dependent conversion. The corresponding median LAS magnitudes were 0.086 and 0.099 μg $m^{-2}$ $s^{-1}$, compared with a dry-deposition median of 0.058 μg $m^{-2}$ $s^{-1}$. Because measured concentration is combined with a parameterized deposition velocity, this calculation is treated as a process-based reference and not as an independent flux validation.

The comparison is reproduced below to show the scale, pairing, and effect of the RH-dependent conversion.

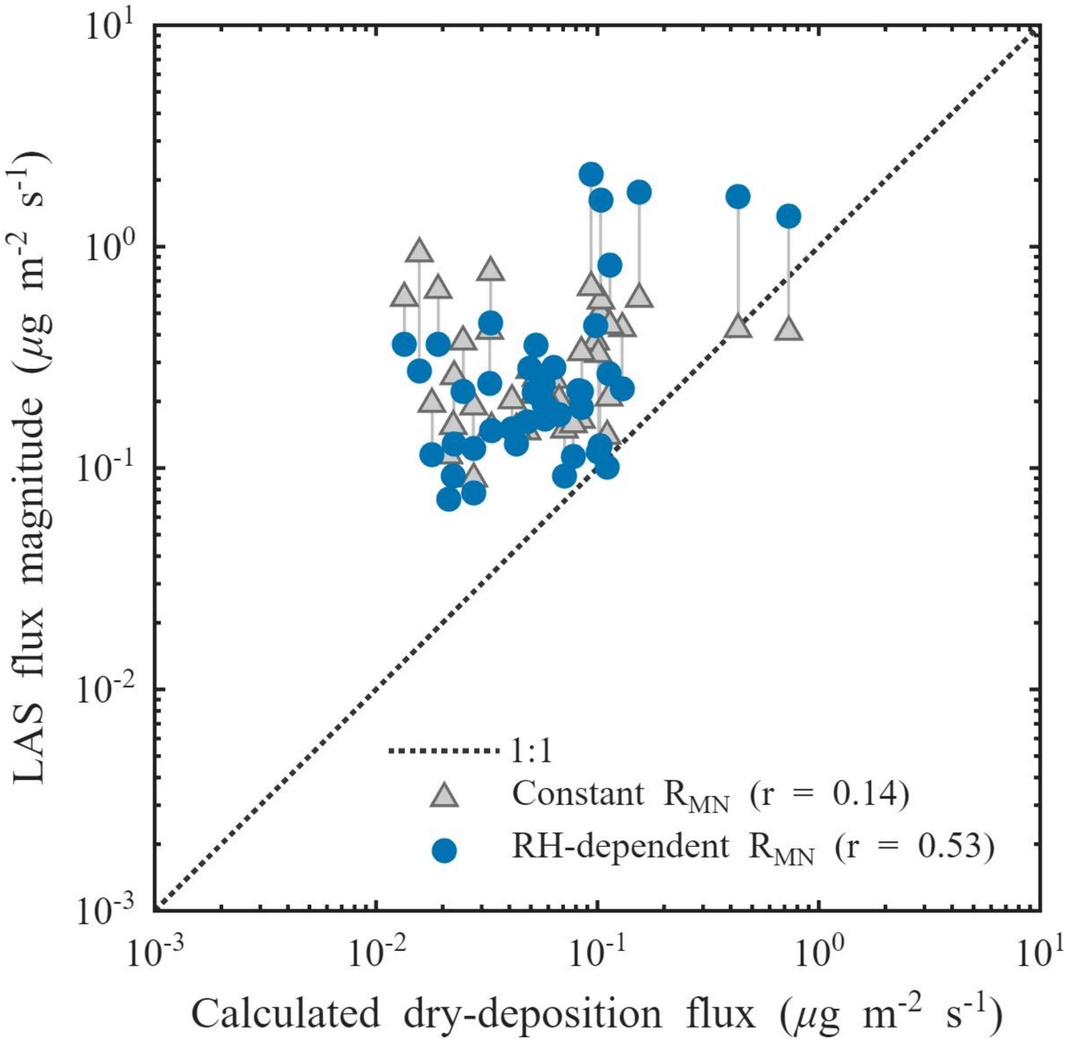


**Figure R5 (reproduced from the revised manuscript Fig. 13).** Comparison of the calculated dry-deposition flux with LAS-derived aerosol mass-flux magnitudes obtained using a constant $R_{MN}$ of 3845 kg m−3 (gray triangles) and the RH-dependent $R_{MN}$ (blue circles). Gray lines connect the two LAS calculations, and the dotted line denotes 1:1 agreement. Both axes are logarithmic.

**The Sect. 2.6, Pages 9-10, lines 221-239:**

"A dry-deposition estimate was constructed as a physical reference for the

LAS-derived aerosol mass-flux magnitude…where the PM2.5 and PM10 terms denote the corresponding concentrations.”

**The Sect. 3.4, Pages 26-27, lines 538-559:**

“The dry-deposition calculation provided an independent reference for the LAS-derived flux magnitude…Both axes are logarithmic.”

**Minor Comment 7:** Explain why the 0.1 mg precision of the analytical balance is sufficient to attain 0.0001 ug precision in the aerosol flux.

**Response:** We agree that the former presentation implied more precision than was supported by the measurement and model inputs. The dry-deposition median is now reported as 0.058 μg $m^{-2}$ $s^{-1}$ rather than to four decimal places. The original manuscript described the EAB 125i balance only as having a precision of 0.1 mg. The revised methods distinguish the manufacturer-specified readability of 0.01 mg, repeatability of 0.03 mg (standard deviation), and linearity of ±0.08 mg within the ≤62 g semi-micro range. They also report the <0.4 mg duplicate-weighing acceptance criterion, the 0.10 mg operational minimum loading, and the 0.042 mg standard uncertainty contribution for the mass difference.

**The Sect. 2.7, Page 11, lines 271-281:**

“Quality control of the filter-based $PM_{2.5}$ and $PM_{10}$ measurements followed the weighing-related provisions of HJ 618-2011…equivalent to 3.6–4.1 μg $m^{-3}$ over the observed range of sampled-air volumes.”

**Minor Comment 8:** Be explicit about point-average and path-average for LAS at heterogeneous surfaces.

**Response:** We thank the reviewer for this guidance. A point measurement is associated with one receptor location and therefore with one upwind footprint. In contrast, the LAS signal contains contributions from turbulence along the entire optical path, and these contributions are not equally weighted. Consequently, the LAS measurement cannot be represented by either a footprint calculated at the path midpoint or an arithmetic average of several point footprints. We calculate a point-receptor FFP footprint at each node along the optical path and integrate these footprints using the normalized scintillometer path-weighting function $W(s)$. The resulting $f_{\mathrm{LAS}}$ therefore represents the spatial sensitivity of the path-integrated LAS retrieval. The corresponding formulation and calculation are described in Sect. 2.5 of the revised manuscript.

To quantify the effect of surface heterogeneity, the water contribution was calculated by overlaying the normalized LAS footprint climatology on the land–water mask:

$$\eta_{\mathrm{water}}=\frac{\iint_{\Omega_{\mathrm{water}}} f_{\mathrm{LAS}}\,(x,y)\;\mathrm{d}x\;\mathrm{d}y}{\iint_{\Omega_{\mathrm{total}}} f_{\mathrm{LAS}}\,(x,y)\;\mathrm{d}x\;\mathrm{d}y}.$$

This analysis shows that water contributed 79.4 % and 75.1 % of the path-weighted footprint during Siyuan Lake I and II, leaving non-negligible land contributions of 20.6 % and 24.9 %, respectively. The lake retrievals are therefore interpreted as spatially integrated flux signals dominated by, but not attributable exclusively to, the water surface. In contrast, water contributed 99.4 % and 99.6 % during Sijiao Island I and II, with corresponding land contributions of only 0.6 % and 0.4 %. The coastal retrievals can therefore be interpreted as representing water-surface exchange almost exclusively.

**The Sect. 2.5, Page 9, lines 204-214:**

"The spatial support of the LAS flux retrievals was quantified with the two-dimensional Flux Footprint Prediction parameterization…with its path integral set to unity."

**Minor Comment 9:** Add a table of equipment used, similar to table 1 for meteorological conditions.

**Response:** We thank the reviewer for this helpful suggestion and have added a table in Section 2.1. Table 1 lists each instrument, manufacturer and model, measured variable, acquisition or response characteristics, and the site-specific deployment geometry. The table also distinguishes recorded logging frequency from an instrument's independent measurement interval or physical response time.

**The Sect. 2.1, Pages 5-6, line 124 (Table 1):**

"Table 1. Specifications, temporal characteristics, and study-specific configuration of the observational instruments…mounting heights are reported relative to the local water surface."

**Minor Comment 10:** Consider adding relevant references to statements made in the introduction that are now lacking references.

**Response:** We thank the reviewer for this constructive suggestion. We have incorporated the relevant references into the Introduction to support our statements. The newly added references have also been included in the reference list.

**Minor Comment 11:** Add information regarding the calibration of the different sensors associated with the sonic anemometer, as they have different sampling frequencies, and thus could sample different volumes of air.

**Response:** We sincerely thank the reviewer for highlighting this critical methodological detail. In the original analysis, we attempted to account for the different sampling frequencies and spatial separation of the sonic anemometer and visibility sensor before calculating the aerosol eddy covariance.

The sonic anemometer and the visibility sensor operate at different sampling frequencies (20 Hz and 1 Hz, respectively) and are physically separated. To align the sampled air volumes, a two-step synchronization procedure was applied prior to the covariance calculation. First, the 20 Hz high-frequency wind velocity data were block-averaged to 1 Hz. This frequency matching induces a negligible high-frequency flux loss (< 5%), which is analytically acceptable for capturing the energy-containing turbulent eddies (Yuan et al., 2024).

Second, to calculate aerosol fluxes using EC techniques, a delayed correlation of the vertical velocity and extinction coefficient is needed. A representative delayed correlation curve after linear detrending is given in Fig. R1. The horizontal coordinate of the delayed correlation curve is the delay time τ, and the vertical coordinate is the covariance. From Fig. R1, it can be seen that the correlation curve has an obvious extreme value $9.356 \times 10^{-7}$ $m^{-1}$ at $\tau = -2$ s, which identifies the optimal time lag for this specific interval. The extreme value of the correlation curve generally does not appear at exactly 0 s because there is a physical distance between the sensing elements of the visibility meter and the ultrasonic anemometer. By dynamically determining this optimal delay time within a physically realistic window for each 30-min interval, the sampled air volumes can be aligned. In cases where no significant extremes appear, the value associated with a delay time of 0 s is taken.

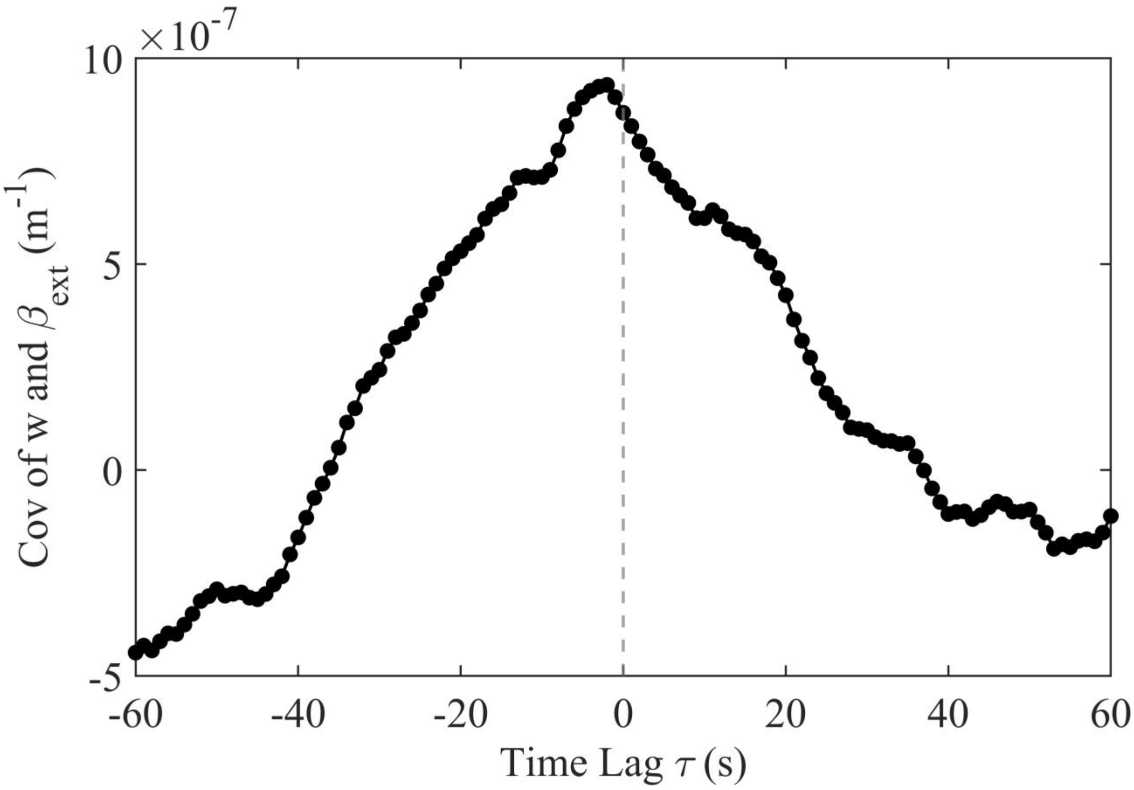


**Figure R6.** Delay covariance between the vertical wind velocity ( $w$ ) and the extinction coefficient ( $\beta_{ext}$ ) during 24 August 2024 11:00-11:30 LST at the first SiYuan Lake campaign.

However, prompted by Reviewer 2's concern regarding the PWD50, we re-examined the instrument's temporal characteristics and the validity of this correction. Although the PWD50 output was recorded at 1 Hz, its independent measurement interval is 15 s. Consecutive 1 s records therefore do not represent independent fast-response extinction observations. Block-averaging the sonic-anemometer data to 1 Hz matched only the recorded timestamps; it did not match the physical response of the two instruments. Similarly, shifting the records according to a covariance extremum could compensate for an apparent advection delay but could not restore the extinction fluctuations attenuated by the PWD50 response or eliminate the difference between the two sensing volumes. In the revised analysis, the two instruments are no longer treated as components of one covariance system.

**Minor Comment 12:** Explain in more detail how the wind directions were selected to reduce flow distortion.

**Response:** We thank the reviewer for this suggestion. Section 2.7 has been revised to provide a detailed explanation of the wind direction sectors excluded to eliminate flow distortion.

**The Sect. 2.7, Page 11, lines 260-265:**

"Particular attention was given to flow distortion caused by the supporting structure…This directional screening was applied before coordinate rotation."

**Minor Comment 13:** Explain to what extent PM10 is a good approximation or proxy for aerosol mass concentration.

**Response:** We thank the reviewer for this comment. Following Yuan et al. (2016, 2019), the operational aerosol mass variable Ma in the LAS conversion is approximated by $PM_{10}$. In addition to maintaining continuity with the preceding LAS aerosol-flux framework, $PM_{10}$ was selected because it provides a defined and reproducible size-selective mass fraction for the empirical conversion between aerosol mass and optical extinction. At the LAS wavelength of 625 nm, accumulation-mode particles (approximately 0.1–1 μm in diameter) and the sub-10 μm coarse fraction included in $PM_{10}$ contribute effectively to visible-light extinction, whereas extinction efficiency per unit mass generally decreases as particle size increases into the super-coarse range (Seinfeld and Pandis, 2016).

Giant sea-spray particles with aerodynamic diameters greater than 10 μm can contribute substantially to total aerosol mass near the water surface. However, their stronger gravitational settling results in shorter atmospheric residence times and pronounced vertical and spatial variability (Lewis and Schwartz, 2004). Including this super-coarse fraction through a total-suspended-particulate measurement could therefore introduce a highly variable mass contribution that is not necessarily represented proportionally by the visibility-derived imaginary refractive index. The $PM_{10}$ size cut consequently provides a practical compromise: it includes both the accumulation mode and an optically active portion of the coarse mode while excluding a super-coarse fraction with a less stable mass-to-optical relationship.

**The Sect. 2.3, Page 7, lines 156-158:**

"Following Yuan et al. (2016, 2019), aerosol mass concentration is approximated as PM10…the atmospheric equivalent refractive index is expressed through the $R_{MN}$"

**Minor Comment 14:** Indicate how many data points are used in the ensemble.

**Response:** The ensemble EC/LAS plots have been removed. For the remaining analysis, Table 3 reports the number of candidate 30 min intervals and final valid LAS-derived aerosol mass-flux retrievals for each campaign. The final flux datasets contain 1,531 of 1,824 intervals (83.9 %), 2,594 of 3,120 intervals (83.1 %), 119 of 259 intervals (45.9 %), and 259 of 265 intervals (97.7 %) for Siyuan Lake I, Siyuan Lake II, Sijiao Island I, and Sijiao Island II, respectively. These values represent the sample sizes used to calculate the campaign-level flux statistics reported in the revised manuscript.